URSI GASS 2021, Rome, Italy, 28 August - 4 September 2021

A Hardware-In-Loop simulation Test-bed for NavIC Reflectometry Experiments

Bushra Ansari*, Sanat K. Biswas
Department of Electronics and Communication Engineering, IIIT Delhi, New Delhi, India

Abstract

Global Navigation Satellite System-Reflectometry (GNSS-R) is a cost-effective remote sensing technique used to study the Earth's geophysical parameters. The Delay Doppler Map (DDM) generated by correlating locally generated GNSS signal with the GNSS signal reflected from the Earth's surface is utilised in a GNSS-R study. In this article, a Hardware-In-Loop (HIL) test-bed for reflectometry simulation involving Navigation using Indian Constellation (NavIC) is presented and verified using theoretical analysis. The radio-frequency NavIC signal is generated by a constellation simulator. The generated signal is acquired by a Software Defined Radio (SDR) and the DDMs are generated using the acquired digital signal. The peak power levels are compared with the theoretical value for the validation of the generated DDM. The trend of the DDM peak power is also studied with varying dielectric constant of the reflecting surface.

1 Introduction

The GNSS-R technique intends to analyze both the direct and reflected multi-path GNSS satellite signals to study the reflecting surface. In GNSS-R technique the satellite signal is received in multi-static or bi-static radar configuration. The GNSS satellites act as transmitters and the GNSS receiver can either be located on a low-earth orbit satellite, at some height from the ground or on-board a UAV. It has already been reported that land and ocean's geophysical parameters like soil moisture [1], vegetation biomass, presence of wetlands and water bodies [2], sea level, and wind speed can be successfully quantified using GNSS-R technique. The reflected signal carries the information about the reflecting surface, in the form of change in SNR, reflected signal power, path delay and carrier phase. The reflected signals are further processed to generate the Delay Doppler Maps (DDM), resulting from different path delays and Doppler shifts due to change in transmitter-surface-receiver geometry [3].

Earlier GNSS-R analysis includes the study of Signal to Noise ratio (SNR) [4] and Delay Waveforms (DW). Delay Waveform is a simplified form of DDM, which is inadequate for studying the effect of noise and specular point's geometry. Recently, several space-borne GNSS-R missions, such as NASA's Cyclone Global Navigation Satellite System (CYGNSS) and UK's TechDemoSat-1 (TDS-1), has allowed the study of Earth's geophysical parameters from DDMs, processed on-board these satellite A study is performed in [5] using the CYGNSS DDMs, and the effect of noise, surface roughness on reflected signal is studied, which is challenging to examine from SNR retrieval methods. In this paper, the development of Hardware-In-Loop (HIL) NavIC simulator is explained. The study and analysis of the DDM generation and its correlation with theoretical reflected power level for NavIC is also presented. The performance of the NavIC simulation setup is evaluated by comparing the trend with the theoretical results. It is observed that there is a difference in the theoretical DDM peak power and the DDM peak power generated by the HIL. The difference is predominantly due to hardware gain mismatch and noise.

Rest of the paper is organised as follows: In section 2, the methodology and concept of DDM are explained. Section 3 describes the Hardware-In-Loop simulator setup and design. Section 4 discusses the Results of DDM and the comparison with theoretical values. Section 5 summarizes the paper outlining future work.

2 Methodology

A GNSS-R receiver acquire power from the surface reflections in addition to the direct GNSS signal that is received directly from the GNSS satellite. The reflected signals directly change signal-to-noise ratio, creating phase delay, frequency shift and amplitude modifications depending on ground reflections' behaviour. Hence, the reflected signal can be used for reflectometry application. The GNSS signal has a certain delay and doppler frequency due to the relative velocity and position of the transmitter and the receiver. The GNSS signal can be processed into the Delay-Doppler Map (DDM) which is the 2D representation of the power/amplitude distribution of the received GNSS signal. The DDM is a function of doppler shifts and delay offset around the specular point. The power distribution of DDM

as a function of delay and doppler can be expressed as [6]:

$$|P(\tau,f)|^2 = \frac{T_i^2 P_t G_t \lambda^2}{(4\pi)^3} \iint_A \frac{G_r(\vec{\rho})}{R_{ts}(\vec{\rho}) R_{rs}(\vec{\rho})} \sigma^{\circ}_{pq} \chi^2(\vec{\rho};\delta\tau,\delta f) d\vec{\rho} \quad (1)$$

where P_t is the transmitted GNSS signal power, T_i is the integration time, λ is the GNSS signal wavelength, G_t and G_r are the transmitter and receiver antenna gain respectively, R_{ts} and R_{rs} is the distance from the transmitter to the specular point and the receiver to the specular point, σ°_{pq} is the bistatic radar coefficient for a particular polarisation pq, and $\chi^2(\vec{\rho};\delta\tau,\delta f)$ is the Woodward Ambiguity Function.

Now, the theoretical coherent power observed by the receiver is defined as [7]:

$$P_p^{coh} = \frac{P_t \lambda^2 G_t G_r}{(4\pi)^2 (R_{ts}+R_{rs})^2} \Gamma_p(\varepsilon_s,\theta_i) \quad (2)$$

where Γ_p is the surface reflectivity for a particular polarization p. The surface reflectivity Γ_p is a function of surface dielectric constant which depends on the reflecting surface, hence the change in reflecting surface properties will affect the coherent reflected power received at the GNSS receiver. The surface reflectivity Γ_p is a function of both surface dielectric constant ε_s and elevation angle θ_i and is defined as [5]:

$$\Gamma_p(\varepsilon_s,\theta_i) = \left|\frac{1}{2}(R_{vv}-R_{hh})\right|^2 \quad (3)$$

where R_{vv} and R_{hh} are fresnel coefficients for vertical and horizontal polarization. Further, the theoretical coherent power levels are calculated using (2) for different values of dielectric constant (i.e.surface properties) and then compared with the power levels obtained from the DDM of the simulated signal. The NavIC signal used in this study is simulated using the GNSS Simulator SIMAC2. The evaluation metric considered for the validation is the peak power levels of the DDM and the theoretical peak power levels.

3 HIL Simulator setup

The simulation of NavIC RF signal is carried out for generating the dataset used in this article. The multipath NavIC signal is simulated for different dielectric constant values using the physics-based approach. The transmitter height for the simulation is 35937360.181 m and the satellite elevation angle is set to 38.6°. The NavIC RF signal is received by the receiver kept at the height of 30 m from the ground. The NavIC signals are simulated for a single satellite, with Psuedo-Random Noise (PRN) code 6. After setting all the variables, the NavIC RF signal is received using the BladeRF SDR. The NavIC signal is then processed to obtain the DDM for all the dielectric constant values used in the study. The HIL simulator testbed setup [8] is shown in Fig. 1.

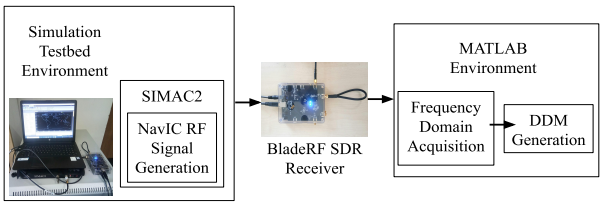

Figure 1. HIL simulator testbed for NavIC DDM generation [8]

4 Results and Discussion

The comparison between the theoretical peak power and the DDM peak power obtained from the RF NavIC signal is presented in this section. The theoretical power levels are calculated using (2), and then the trend of peak power levels is observed with respect to the increasing value of dielectric constant as shown in Fig. 2.

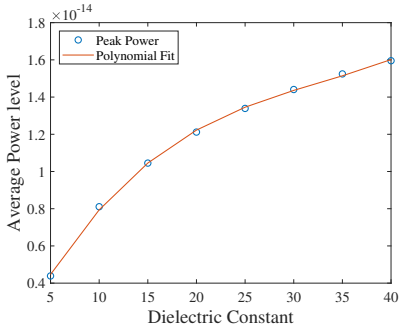

Figure 2. Theoretical Peak power level trend w.r.t dielectric constant

The Fig. 2 shows an increasing trend with increase in the dielectric values. The peak power levels are also obtained from the DDMs generated using simulated NavIC RF signal. The example of DDM for dielectric constant 40 and satellite PRN 6 is shown in Fig. 3. The correlation values depicted in Fig. 3 are in arbitrary counts.

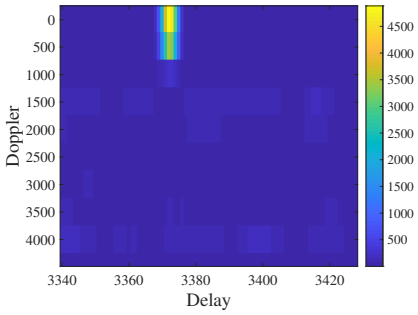

Figure 3. NavIC-DDM Example

After computing the DDMs, the peak power levels are extracted and observed with the increasing dielectric constant.

Fig. 4 depicts the trend of DDM peak power with respect to the dielectric constant.

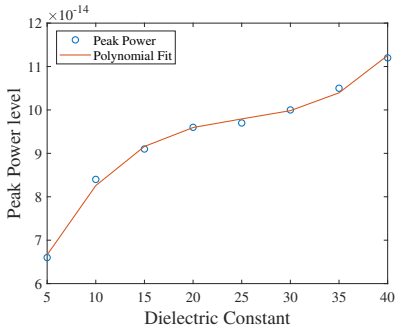

Figure 4. DDM Peak power level trend w.r.t dielectric constant

As expected, the DDM peak power levels generated from the HIL test-bed increases with the increase in the dielectric constant. The peak power levels for theory and the test-bed are fitted to 3rd order polynomial. Although the values of the theoretical and the experimental peak power are different, the peak power levels show similar trends. The difference between the peak power levels is presented in Fig. 5. The error remains within the range of 6.2×10^{-14} to 9.6×10^{-14}. The peak power levels in Fig. 5 are depicted in semilog axis. From Fig. 5 it is observed that there are some discrepancies between the theoretical and DDM peak power levels. The average error between the theoretical and peak power levels obtained from the HIL simulation is 13% .The effect of noise, internal delays in the hardware and gain mismatch contributes to the error between the theoretical and the HIL simulation observation.

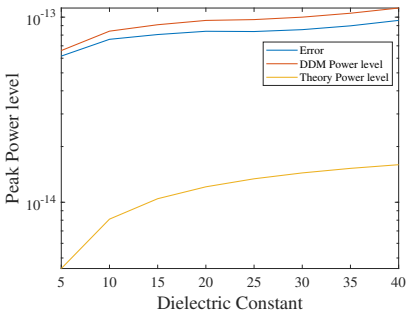

Figure 5. Error between the Theoretical and DDM Peak power levels

5 Conclusion

A HIL simulation test-bed for NavIC reflectometry experiments is presented. The DDM peak power level obtained using the HIL setup is compared with the theoretical peak power. The comparison shows a good agreement between the theoretical peak power and the HIL generated peak power, with 13% average error. The effect of the increase in dielectric constant value on DDM peak power levels is also observed. Future work is focused on detailed verification of the experimental DDM obtained using the NavIC reflectometry HIL test-bed, considering the effect of noise, surface roughness, internal delay in hardware and gain mismatch.

6 Acknowledgement

The work is partially supported by the Institute Research Grant, IIIT Delhi and DST-SERB Early Career Research Award (ECR/2018/001492).

References

[1] M. P. Clarizia, N. Pierdicca, F. Costantini, and N. Floury, "Analysis of cygnss data for soil moisture retrieval," *IEEE Journal of Selected Topics in Applied Earth Observations and Remote Sensing*, vol. 12, no. 7, pp. 2227–2235, 7 2019.

[2] C. Zuffada, C. Chew, and S. V. Nghiem, "Global Navigation Satellite System Reflectometry (GNSS-R) algorithms for wetland observations," in *International Geoscience and Remote Sensing Symposium (IGARSS)*, 2017.

[3] J. Park, J. T. Johnson, A. O'Brien, and S. T. Lowe, "Studies of TDS-1 GNSS-R ocean altimetry using a 'full DDM' retrieval approach," in *International Geoscience and Remote Sensing Symposium (IGARSS)*, 2016.

[4] K. M. Larson, E. E. Small, E. Gutmann, A. Bilich, P. Axelrad, and J. Braun, "Using GPS multipath to measure soil moisture fluctuations: Initial results," *GPS Solutions*, 2008.

[5] M. M. Al-Khaldi, J. T. Johnson, A. J. O'Brien, A. Balenzano, and F. Mattia, "Time-Series Retrieval of Soil Moisture Using CYGNSS," *IEEE Transactions on Geoscience and Remote Sensing*, vol. 57, no. 7, pp. 4322–4331, 7 2019.

[6] b. Alejandro Egido Egido, G. Ruffini Forés Starlab Barcelona, and A. José Camps Carmona, "GNSS Reflectometry for Land Remote Sensing Applications," Tech. Rep., 2013.

[7] Y. Jia, P. Savi, Y. Pei, and R. Notarpietro, "GNSS reflectometry for remote sensing of soil moisture," in *2015 IEEE 1st International Forum on Research and Technologies for Society and Industry, RTSI 2015 - Proceedings*. Institute of Electrical and Electronics Engineers Inc., 11 2015, pp. 498–501.

[8] B. Ansari, V. Kaushik, and S. K. Biswas, "Raw GNSS Data Compression using Compressive Sensing for Reflectometry Applications," in *2020 33rd General Assembly and Scientific Symposium of the International Union of Radio Science, URSI GASS 2020*. Institute of Electrical and Electronics Engineers Inc., 8 2020.